Improving the Characteristics of Rectangular Waveguide Branchings by Cylindrical Obstacles

ROLAND GESCHE, MEMBER, IEEE, AND STEPHAN RUSSENSCHUCK, MEMBER, IEEE

Abstract—**The scattering matrix of a transition between one or two parallel rectangular waveguides and a larger rectangular waveguide which contains two metallic or dielectric cylinders is investigated by means of the orthogonal expansion method. Mathematical programming is applied in order to improve the characteristics. Reflection of a rectangular step discontinuity can be reduced by 30 dB using metallic or dielectric obstacles. Using Teflon cylinders, coupling of a transition can be reduced by 40 dB without debasing reflection. Physical interpretations are given with the help of field patterns.**

I. Introduction

RECTANGULAR waveguide branchings are used in many microwave applications. Mode-coupling structures which are used in satellite stabilization systems are discussed in [1] and [2], while multimode antenna sources and mode selectors are discussed in [3]. The quality of these structures is dependent on the reflection coefficients in the feeding waveguides and the coupling coefficients between adjoining transmitting and receiving waveguides. It is possible to minimize the scattering coefficients by placing cylindrical obstacles near the waveguide inhomogeneities.

In this paper, the structure shown in Fig. 1 is investigated considering the following restrictions:

- incident fields are TE_{m0} modes;
- the axes of the cylindrical obstacles are parallel to the electric field vector;
- the obstacles are made of ideal conducting materials or of lossy dielectric materials which are linear, homogeneous, and isotropic;
- the obstacles extend over the entire waveguide height;
- the axes of both obstacles are placed in the same cross section of the larger waveguide; and
- all waveguide walls are ideally conducting.

By means of the orthogonal expansion method [4], the scattering parameters are determined in a reliable way.

Manuscript received July 27, 1987; revised April 18, 1989.

R. Gesche is with Leybold AG, Siemensstr. 100, 8755 Alzenau, West Germany.

S. Russenschuck is with the Institute of Electrical Energy Conversion, Technical University of Darmstadt, 6100 Darmstadt, West Germany.

IEEE Log Number 8929896.

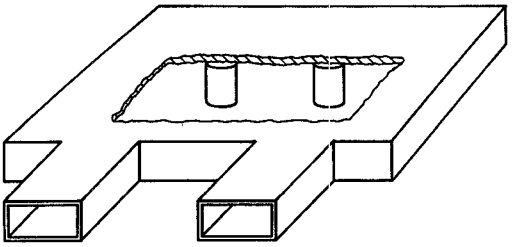

Fig. 1. Waveguide branching with two cylindrical obstacles.

II. Mathematical Method

The investigation of the present structure as shown in Fig. 2 is done in three steps:

A) investigation of the rectangular waveguide branching without obstacles;
B) investigation of the scattering by two cylindrical obstacles in a rectangular waveguide; and
C) determination of the scattering matrix of the complete structure by combination of the scattering matrices from A) and B).

The mathematical formulations of these three steps are described in [4]–[9]. Therefore, a summation of the main equations will be given in this paper. The structure is divided into four waveguide regions, W1–W4, as shown in Fig. 2 indicated by the indices (1)–(4). In each region, the fields of the incident TE_{m0} mode and all scattered fields are independent of z and can be derived from a vector potential:

$$\vec{A}^{(\iota)} = A_z^{(\iota)} \vec{e}_z e^{j\omega t} \qquad \vec{H}^{(\iota)} = \nabla \times \vec{A}^{(\iota)}$$

$$\vec{E}^{(\iota)} = \frac{1}{j\omega\epsilon_0}\left(\nabla \times \vec{H}^{(\iota)}\right) \tag{1}$$

$$A_z^{(\iota)} = \sum_{m=1}^{\infty} g^{(\iota)} \sin k_{ym}^{(\iota)}\left(y - s^{(\iota)}\right)\left\{ f_m^{(\iota)} e^{-jk_{xm}^{(\iota)} x} + r_m^{(\iota)} e^{+jk_{xm}^{(\iota)} x} \right\} \tag{2}$$

$$g^{(\iota)} = \frac{2}{\sqrt{h^{(\iota)}}} \qquad k_{ym}^{(\iota)} = \frac{m\pi}{h^{(\iota)}} \qquad k_{xm} = \sqrt{\omega^2 \mu_0 \epsilon_0 - k_{ym}^2}\,. \tag{3}$$

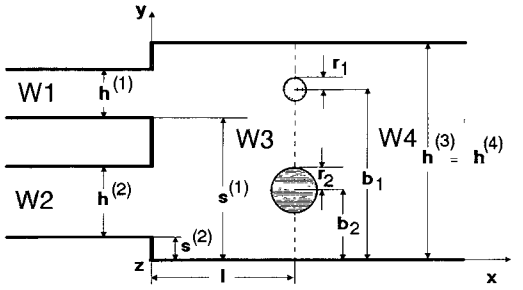

Fig. 2 Geometry of the investigated structure.

A. Waveguide Branching Without Obstacles

The scattering problem of a branching of three rectangular waveguides can be solved by the orthogonal expansion method described in [4]. Special formulations for the present problem are given in [3] and [5]. The following abbreviations are introduced:

$$L_m^{(\iota)} = \left(f_m^{(\iota)} + r_m^{(\iota)}\right)\frac{\omega^2\epsilon_0\mu_0}{j\omega\epsilon} \qquad M_m^{(\iota)} = \left(f_m^{(\iota)} + r_m^{(\iota)}\right) jk_{xm}^{(\iota)}$$

$$\Phi_m^{(\iota)} = g^{(\iota)} \sin k_{ym}^{(\iota)}\left(y - s^{(\iota)}\right). \tag{4}$$

The equation arising from the continuity condition for the tangential electrical field component E_z is multiplied by $\Phi_m^{(3)}$ and integrated over the surface $x = 0$. Using the orthogonality relation, it follows that

$$\sum_{n=1}^{\infty} L_n^{(1)} \int_{s^{(1)}}^{s^{(1)} + h^{(1)}} \Phi_n^{(1)} \Phi_m^{(3)}\, dy + \sum_{p=1}^{\infty} L_p^{(2)} \int_{s^{(2)}}^{s^{(2)} + h^{(2)}} \Phi_p^{(2)} \Phi_m^{(3)}\, dy = L_m^{(3)}. \tag{5}$$

The similar equation coming from the continuity condition for the tangential magnetic field component H_y is multiplied by $\Phi_m^{(1)}$ and $\Phi_m^{(2)}$. After integration,

$$\sum_{m=1}^{\infty} M_m^{(3)} \int_{s^{(1)}}^{s^{(1)} + h^{(1)}} \Phi_m^{(3)} \Phi_n^{(1)}\, dy = M_n^{(1)}$$

$$\sum_{m=1}^{\infty} M_m^{(3)} \int_{s^{(2)}}^{s^{(2)} + h^{(2)}} \Phi_m^{(3)} \Phi_n^{(2)}\, dy = M_n^{(2)}. \tag{6}$$

The coupling integrals are arranged in matrices:

$$\underline{F} = (F_{mn}) \qquad F_{mn} = \int_{s^{(1)}}^{s^{(1)} + h^{(1)}} \Phi_m^{(3)} \Phi_n^{(1)}\, dy$$

$$\underline{G} = (G_{mp}) \qquad G_{mp} = \int_{s^{(2)}}^{s^{(2)} + h^{(2)}} \Phi_m^{(3)} \Phi_p^{(2)}\, dy. \tag{7}$$

The amplitudes are arranged in vectors:

$$\vec{f}^{(\iota)} = \begin{bmatrix} f_1^{(\iota)} \\ f_2^{(\iota)} \\ \vdots \end{bmatrix} \qquad \vec{r}\,(i) = \begin{bmatrix} r_1^{(i)} \\ r_2^{(i)} \\ \vdots \end{bmatrix}. \tag{8}$$

Using (7) and (8), (5) and (6) yield

$$\begin{bmatrix} 1 & -\underline{F} & -\underline{G} \\ \underline{K}^{(3)} \cdot \underline{F} & \underline{K}^{(1)} & \underline{0} \\ \underline{K}^{(3)} \cdot \underline{G} & \underline{0} & \underline{K}^{(2)} \end{bmatrix} \cdot \begin{bmatrix} \vec{f}^{(3)} \\ \vec{r}^{(1)} \\ \vec{r}^{(2)} \end{bmatrix} = \begin{bmatrix} -1 & \underline{F} & \underline{G} \\ \underline{K}^{(3)} \cdot \underline{F} & \underline{K}^{(1)} & \underline{0} \\ \underline{K}^{(3)} \cdot \underline{G} & \underline{0} & \underline{K}^{(2)} \end{bmatrix} \cdot \begin{bmatrix} \vec{r}^{(3)} \\ \vec{f}^{(1)} \\ \vec{f}^{(2)} \end{bmatrix}$$

$$\underline{K}^{(\iota)} = \operatorname{diag}\left(k_{xm}^{(\iota)}\right). \tag{9}$$

The scattering matrix can be calculated from (9):

$$\begin{bmatrix} \vec{f}^{(3)} \\ \vec{r}^{(1)} \\ \vec{r}^{(2)} \end{bmatrix} = \underline{S}_1 \cdot \begin{bmatrix} \vec{r}^{(3)} \\ \vec{f}^{(1)} \\ \vec{f}^{(2)} \end{bmatrix} \tag{10}$$

$$\underline{S}_1 = \begin{bmatrix} 1 & -\underline{F} & -\underline{G} \\ \underline{K}^{(3)} \cdot \underline{F} & \underline{K}^{(1)} & \underline{0} \\ \underline{K}^{(3)} \cdot \underline{G} & \underline{0} & \underline{K}^{(2)} \end{bmatrix}^{-1} \cdot \begin{bmatrix} -1 & \underline{F} & \underline{G} \\ \underline{K}^{(3)} \cdot \underline{F} & \underline{K}^{(1)} & \underline{0} \\ \underline{K}^{(3)} \cdot \underline{G} & \underline{0} & \underline{K}^{(2)} \end{bmatrix}. \tag{11}$$

B. Two Cylindrical Obstacles in a Rectangular Waveguide

The investigation of the scattering of two cylindrical obstacles in a rectangular waveguide is described in [7] and [8] and can be omitted here:

$$\begin{bmatrix} \vec{r}^{(3)} \\ \vec{f}^{(4)} \end{bmatrix} = \underline{S}_2 \begin{bmatrix} \vec{f}^{(3)} \\ \vec{r}^{(4)} \end{bmatrix} \tag{12}$$

$$\underline{S}_2 = \begin{bmatrix} \underline{T} & \underline{0} \\ \underline{0} & \underline{T}^{-1} \end{bmatrix} \underline{S} \begin{bmatrix} \underline{T} & \underline{0} \\ \underline{0} & \underline{T}^{-1} \end{bmatrix} \tag{13}$$

$$\underline{T} = \operatorname{diag}\left[e^{-jk_x^{(3)}l}\right] \qquad \text{transformation matrix} \tag{14}$$

$\underline{S}$ is the scattering matrix from [8].

C. Combining the Scattering Matrices from A and B

The complete structure consists of the two discontinuities A and B coupled by the rectangular waveguide region W3. The amplitudes of the H_{m0} modes in the coupling waveguide combine the scattering matrices. Equation (10) yields

$$\begin{bmatrix} \vec{f}^{(3)} \\ \vec{r}^{(1)} \\ \vec{r}^{(2)} \end{bmatrix} = \begin{bmatrix} \underline{S}_{1a} & \underline{S}_{1b} \\ \underline{S}_{1c} & \underline{S}_{1d} \end{bmatrix} \cdot \begin{bmatrix} \vec{r}^{(3)} \\ \vec{f}^{(1)} \\ \vec{f}^{(2)} \end{bmatrix}. \tag{15}$$

Equation (12) yields

$$\begin{bmatrix} \vec{r}^{(3)} \\ \vec{f}^{(4)} \end{bmatrix} = \begin{bmatrix} \underline{S}_{2a} & \underline{S}_{2b} \\ \underline{S}_{2c} & \underline{S}_{2d} \end{bmatrix} \cdot \begin{bmatrix} \vec{f}^{(3)} \\ \vec{r}^{(4)} \end{bmatrix}. \tag{16}$$

Now the amplitudes of the coupling region W3 are elimi-

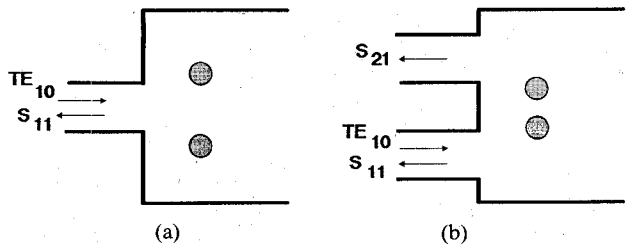

Fig. 3. Structures to be optimized. (a) Step discontinuity: $h^{(1)} = h =$ normalization length, $s^{(1)} = 2h$, $h^{(2)} = 0$, $s^{(2)} = 0$, $h^{(3)} = h^{(4)} = 5h$. (b) Waveguide branching: $h^{(1)} = h =$ normalization length, $s^{(1)} = 3.5h$, $h^{(2)} = h$, $s^{(2)} = 0.5h$, $h^{(3)} = h^{(4)} = 5h$. The post size and location are to be optimized. Symmetric structures with $b_2 = h^{(3)} - b_1$, $r_2 = r_1$.

nated. It follows that

$$\begin{bmatrix} \vec{r}^{(1)} \\ \vec{r}^{(2)} \\ \vec{f}^{(4)} \end{bmatrix} = \begin{bmatrix} \underline{S}_a & \underline{S}_b \\ \underline{S}_c & \underline{S}_d \end{bmatrix} \cdot \begin{bmatrix} \vec{f}^{(1)} \\ \vec{f}^{(2)} \\ \vec{r}^{(4)} \end{bmatrix} \tag{17}$$

$$\begin{aligned} \underline{S}_a &= \underline{S}_{1c} \cdot \left(\underline{E} - \underline{S}_{2a}^T \cdot \underline{S}_{1a}^T \right)^{-1} + \underline{S}_{1d} \\ \underline{S}_b &= \underline{S}_{1c} \cdot \left(\underline{E} - \underline{S}_{2a}^T \cdot \underline{S}_{1a}^T \right)^{-1} \cdot \underline{S}_{2b} \\ \underline{S}_c &= \underline{S}_{2c} \cdot \underline{S}_{1b} + \underline{S}_{2c} \cdot \underline{S}_{1a} \cdot \left(\underline{E} - \underline{S}_{2a} \cdot \underline{S}_{1a} \right)^{-1} \cdot \underline{S}_{2a} \cdot \underline{S}_{1b} \\ S_d &= \underline{S}_{2d} \cdot \left(\underline{E} - \underline{S}_{2a} \cdot \underline{S}_{1a} \right) \cdot \underline{S}_{2b} \end{aligned} \tag{18}$$

where $\underline{E}$ is the unity matrix.

III. Optimization

Because of the number of possible design variables, the application of mathematical optimization algorithms is recommended. Fig. 3 shows the two structures that are discussed in the following.

A. Step Discontinuity

In the case of the step discontinuity (Fig. 3(a)), the optimization problem is obvious:

$$\text{minimize } f(\vec{X}) \qquad \vec{X} \in \mathbb{R} \qquad f: \mathbb{R}^n \to \mathbb{R} \tag{19}$$

subject to

$$\vec{g}(\vec{X}) \leqslant \vec{\theta}_m \qquad \vec{g}: \mathbb{R}^n \to \mathbb{R}^m \tag{20}$$

with the set of real numbers $\mathbb{R}$, the objective function $f(\vec{X}) = S_{11}(\vec{X})$, the vector of design variables $\vec{X} = (l, b_1, r_1) \in \mathbb{R}$, the zero vector $\vec{\theta}_{m,p}$, and the feasible domain

$$R = \left\{ \vec{X} \in \mathbb{R}^n | \vec{g}(\vec{X}) \leqslant \vec{\theta}_m \right\} \tag{21}$$

of $\vec{X}$ for which the nonequality constraints (20) are satisfied. In the particular case the feasible domain is given by

$$R = \left\{ \vec{X} \in \mathbb{R}^3 | 0.25h \leqslant 1 \leqslant 2h,\ h \leqslant b_1 \leqslant 4.75h,\ 0.025h \leqslant r_1 \leqslant 0.2h \right\}. \tag{22}$$

A global minimum point $\vec{X}^* \in \mathbb{R}^n$ is characterized by

$$f(\vec{X}^*) \leqslant f(\vec{X}) \qquad \forall\, \vec{X} \in R. \tag{23}$$

As continuity, differentiability, and convexity of the objective function cannot be determined because it is not given analytically, the minimum conditions cannot be verified. The characteristic of nonconvex problems is the possibility of the appearance of multiple minima. A minimum found by an algorithm has therefore to be tested to determine whether it is global by using a number of starting vectors. Because of the periodical structure of traveling waves, multiple local minima in the feasible domain have been found. As the constraints are nonactive in the minima, the optimization problem can be treated as an unconstrained optimization problem when the search is performed from the inside of the feasible domain. The published algorithms for nonlinear unconstrained minimization problems [10]–[12] can be used, but efficiency tests should be carried out for the optimization problems presented, because the algorithms have a problem-dependent efficiency [10]. As zeroth-order algorithms (search algorithms), where only the objective function value is desired, the

- direct search method with unidimensional Coggin algorithm,
- pattern search by Hooke and Jeeves,
- flexible polyhedron search by Nelder and Mead,
- algorithm EXTREM by Jacob,
- Rosenbrock algorithm, and
- Powell algorithm

have been chosen for testing, as well as the quasi-Newton method established by Davidon-Fletcher Powell.

Quasi-Newton methods, also termed variable metric methods, approximate the Hessien matrix but use information only from first-order derivatives to do so.

Defining efficiency as a weighted function of criteria such as convergence behavior (number of function evaluations to find the minimum), robustness (success in obtaining a solution without problem-dependent parameters), accuracy, and user's comfort (easy to program and to apply), the quasi-Newton method, which shows a good convergence when applied to mathematical test functions such as the Rosenbrock function [10], loses its advantages because the gradient of the objective function has to be approximated numerically by a difference quotient where the spacing is computer and very much problem dependent when f is covered with errors. The Nelder–Mead algorithm performed rather poorly on our problem because it had to be restarted after about every 20th cycle with a different user-supplied length of the starting simplex.

In Fig. 4 the numbers of function evaluations dependent on the logarithm of the difference between the objective function values at the actual and the minimum point, $\vec{X}^* = (l = 1.025h,\ b_1 = 3.775h,\ r_1 = 0.068h)$ for the optimization problem of a rectangular step discontinuity with metallic posts are given for the different algorithms. The starting vector is chosen as $\vec{X}_0 = (l = 1.5h,\ b_1 = 4h,\ r_1 = 0.1h)$. The initial step in the search routines is chosen as $\Delta\vec{X} = 0.1(l_u - l_l, b_{1u} - b_{1l}, r_{1u} - r_{1l})$ where the subscripts u

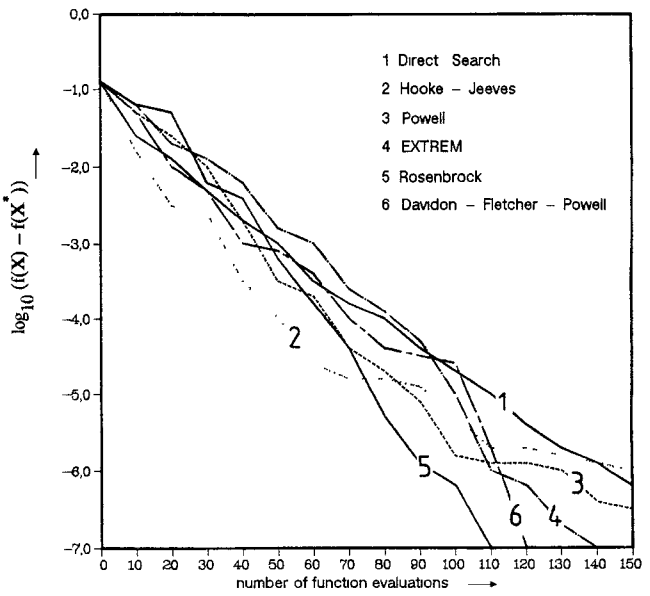

Fig. 4 Convergence behavior of optimization algorithms.

and l denote the upper and the lower bound of the design variables.

Taking robustness and user comfort into consideration, the Rosenbrock algorithm remains most efficient in the present case. The results presented in Section IV are obtained using this algorithm.

B. Waveguide Branching

The rectangular waveguide branching (Fig. 3(b)) is an optimization problem with two objectives where both reflection and transition should be minimized. These problems are called vector optimization problems (VOP's):

$$\text{minimize } \vec{f}(\vec{X}) \qquad \vec{X} \in \mathbb{R}^n \qquad f: \mathbb{R}^n \to \mathbb{R}^k \quad (24)$$

subject to

$$\vec{g}(\vec{X}) \leqslant \vec{\theta}_m \qquad g: \mathbb{R}^n \to \mathbb{R}^m. \quad (25)$$

In the investigated case the feasible domain is given by

$$R = \{ X \in \mathbb{R}^3 | 0.25h \leqslant l \leqslant 2h,\ 3h \leqslant b_1 \leqslant 4.75h,\ 0.025h \leqslant r_1 \leqslant 0.2h \}. \quad (26)$$

Characteristic of such problems is the appearance of an objective conflict where the individual solutions for each single objective function differ and no solution vector $\vec{X}^*$ exists where both objectives gain their individual minimum. In this case, solution points are defined as points where the value of at least one objective function cannot be reduced without increasing the functional values of the other components. These solutions are called Pareto optima [13].

A vector $\vec{X}^* \in \mathbb{R}$ is then and only then Pareto optimal or functional-efficient for the problem (24) if there exists no vector $\vec{X} \in \mathbb{R}$ with

$$\vec{f}_i(\vec{X}) \leqslant \vec{f}_i(\vec{X}^*) \qquad \forall\, i \in \{1, \cdots, k\}$$

and

$$\vec{f}_j(\vec{X}) < \vec{f}_j(\vec{X}^*) \qquad \text{for at least one } j \in \{1, \cdots, k\}. \quad (27)$$

All vectors $\vec{X}^*$ being Pareto optimal build the Pareto optimal solution set $L(\vec{X}^*)$. The decision maker has to choose a compromise solution out of such a solution set. With the preference relation $\lesssim$ defined on L (read $\vec{f}(\vec{X}_1^*) \lesssim \vec{f}(\vec{X}_2^*)$ as $\vec{f}(\vec{X}_1^*)$ is less preferred or indifferent to $\vec{f}(\vec{X}_2^*)$) with

$$\begin{aligned} &\vec{f}(\vec{X}^*) \lesssim \vec{f}(\vec{X}^*) \qquad \forall\, X^* \in L \\ &\vec{f}(\vec{X}_1^*) \lesssim \vec{f}(\vec{X}_2^*) \quad \text{and} \\ &\vec{f}(\vec{X}_2^*) \lesssim \vec{f}(\vec{X}_3^*) \to \vec{f}(\vec{X}_1^*) \lesssim \vec{f}(\vec{X}_3^*) \\ &\vec{f}(\vec{X}_1^*) \lesssim \vec{f}(\vec{X}_2^*) \quad \text{and} \\ &\vec{f}(\vec{X}_2^*) \lesssim \vec{f}(\vec{X}_1^*) \to \vec{f}(\vec{X}_1^*) = \vec{f}(\vec{X}_2^*) \end{aligned} \quad (28)$$

it can be proved [13] that there exists a preference function $p(\vec{f}(\vec{X}))$ with a unique solution $\tilde{X} \in L(\vec{X}^*)$ of the scalarized substitute problem

$$\min p\left(f(\vec{X})\right) \qquad \vec{X} \in \mathbb{R}. \quad (29)$$

Methods for transforming VOP's into substitute problems have been developed such as the method of objective weighting, the distance function method, and the min–max formulation or the Marglin method. The Marglin method transforms the VOP into a scalar substitute problem by minimizing only one of the objective functions while restricting the others with upper bounds. An efficient use of this method requires effective constraint optimization algorithms. In this paper the method of objective weighting is used, defining a preference function

$$p\left(\vec{f}(\vec{X})\right) = \left[w_j f_j(\vec{X})\right] \quad (30)$$

where

$$0 \leqslant w_j \leqslant 1 \quad \text{and} \quad \Sigma w_j = 1 \quad (31)$$

are the weighting factors of the components of the objective function vector $\vec{f}(\vec{X})$. To gain better sensitivity of the weighting factors, the $f_j(\vec{X})$ are related to the components of the function vector of the rectangular waveguide branching without obstacles. The preference function used in this paper reads

$$p\left(\vec{f}(\vec{X})\right) = 0.7\frac{|S_{11}|}{|S_{11}|_0} + 0.3\frac{|S_{21}|}{|S_{21}|_0} \quad (32)$$

where S_{11} is the reflection coefficient in waveguide 1, and S_{21} is the transition coefficient from waveguide 1 to 2. The subscript 0 indicates the coefficients in the branching without obstacles. In this case, the preference function value is equal to 1; every lower value is an improvement.

IV. Results

For the structures investigated in this section, the following definitions are chosen. The small feeding waveguide of the step discontinuity and the branching are chosen as an R-100 waveguide with the width $h = 22.86$ mm $= 9/10$ in. The cutoff frequency of the fundamental TE_{10} mode is 6.56 GHz. Results are given in the frequency range 9.5–10.5 GHz. All dimensions are normalized with respect to the waveguide height h. The larger waveguide has the width $5h$, so the investigated frequency range lies between the

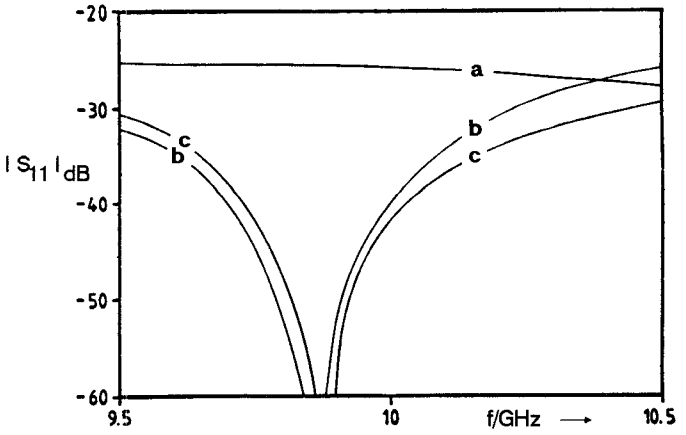

Fig. 5. Reflection coefficient of a symmetric rectangular waveguide step discontinuity (Fig. 3(a)). *a*: without posts. *b*: with two metallic posts: $\epsilon_1 = \epsilon_2 = -j\infty$, $r_1 = r_2 = 0.068h$, $b_1 = 3.775h$, $b_2 = 1.225h$, $l = 1.025h$, $h^{(4)} = 5h$. *c*: with two Teflon posts: $\epsilon_1 = \epsilon_2 = 2.1\epsilon_0$, $r_1 = r_2 = 0.0835h$, $b_1 = 3.105h$, $b_2 = 1.895h$, $l = 0.98h$, $h^{(4)} = 5h$.

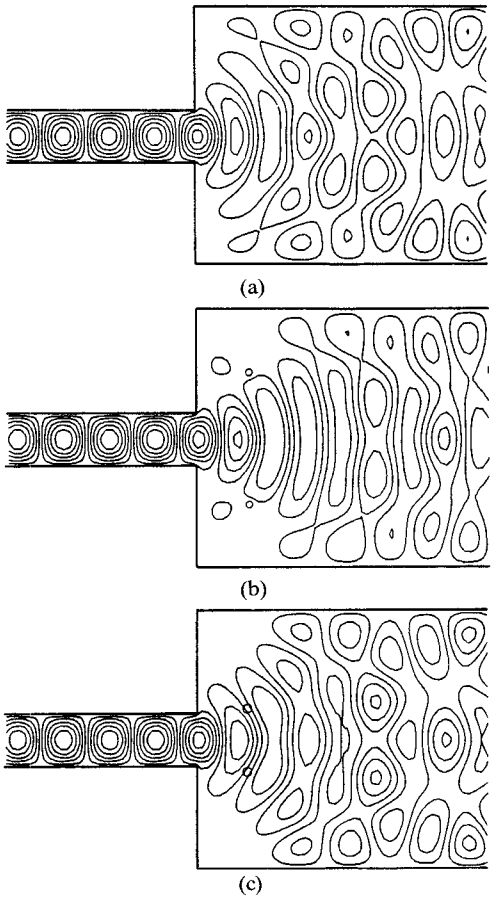

Fig. 6. Magnetic field in the symmetric rectangular step discontinuity from Fig. 3(a) and Fig. 5 at $f = 9.84$ GHz. (a) Without posts: $|S_{11}| = -25$ dB. (b) With two metallic posts: $|S_{11}| = -65$ dB. (c) With two Teflon posts: $|S_{11}| = -55$ dB.

cutoff frequencies of the TE_{70} mode (9.18 GHz) and the TE_{80} mode (10.50 GHz) of the larger waveguide where inhomogeneities of the scattering parameters occur.

A. Rectangular Waveguide Step Discontinuity

Fig. 5 shows frequency responses of the TE_{10} reflection coefficient of a symmetric rectangular waveguide discontinuity. It is obvious that reflection can be reduced by either

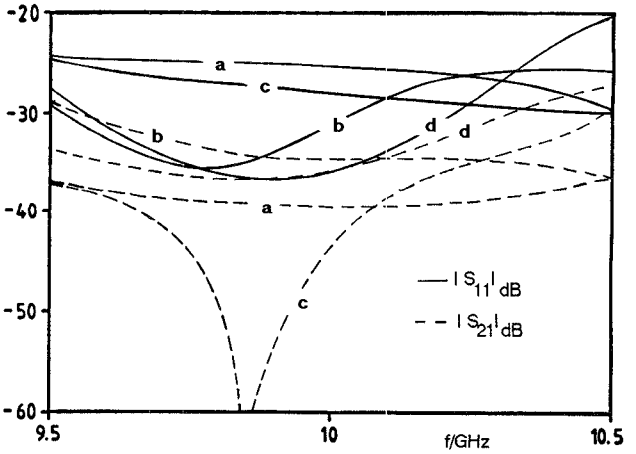

Fig. 7. Reflection and coupling coefficients of a symmetric rectangular waveguide branching. Weighting factors: *a*–*c*: $w_1 = 0.7$, $w_2 = 0.3$; *d*: $w_1 = 0.99$, $w_2 = 0.01$. *a*: without posts $p(\vec{f}(\vec{X}^*)) = 1$. *b*: with two metallic posts: $\epsilon_1 = \epsilon_2 = -j\infty$, $r_1 = r_2 = 0.057h$, $b_1 = 2.8125h$, $b_2 = 2.1875h$, $l = 1.15h$, $h^{(4)} = 5h$, $p(\vec{f}(\vec{X}^*)) = 0.71$. *c*: with two Teflon posts: $\epsilon_1 = \epsilon_2 = 2.1\epsilon_0$, $r_1 = r_2 = 0.084h$, $b_1 = 2.915h$, $b_2 = 2.085h$, $l = 1.491h$, $h^{(4)} = 5h$, $p(\vec{f}(\vec{X}^*)) = 0.7$. *d*: with two asymmetric Teflon posts: $\epsilon_1 = \epsilon_2 = 2.1\epsilon_0$, $r_1 = 0.11h$, $r_2 = 0.191h$, $b_1 = 2.97h$, $b_2 = 2.1h$, $l = 1.45h$, $h^{(4)} = 5h$, $p(\vec{f}(\vec{X}^*)) = 0.5$.

metallic or dielectric posts placed in the large waveguide near the discontinuity. The improvement of reflection becomes greater than 30 dB at 9.86 GHz. Dimensions for optimal reflection coefficients are dependent on step height and frequency. Teflon posts have to be placed closer to the waveguide center.

Although the frequency responses of the metallic and the dielectric post of Fig. 5 look similar, there are differences in the physical mechanism shown by the magnetic fields (Fig. 6). In the feeding waveguide, the incoming TE_{10} mode is dominant in all three cases. Differences are shown by the fields in the large waveguide. The metallic posts split a partial wave from the outward-traveling wave to the transversal direction. This wave is reflected by the waveguide walls and forms a standing wave. Interaction between this standing wave and the outward-traveling wave reduces reflection. The dielectric posts attract the field, so the energy flow is concentrated in the center of the waveguide. The field strength at the discontinuity walls becomes small and the detachment of the fields at the corners is improved, so the reflection is reduced. In all three cases, the amplitudes of the wave mixture in the large waveguide are different.

B. Rectangular Waveguide Branching

Fig. 7 shows the frequency responses of the TE_{10} reflection and coupling coefficients in a symmetric waveguide branching. With metallic posts, reflection can be reduced in a small range, but the coupling increases. Better results are obtained using Teflon posts. The curves show an improvement of coupling with about constant reflection. In other investigated cases, the reflection could be reduced without increasing coupling.

Magnetic field patterns are shown in Fig. 8. In the case of metallic posts, coupling increases because of the greater fields near the discontinuity caused by the transversal

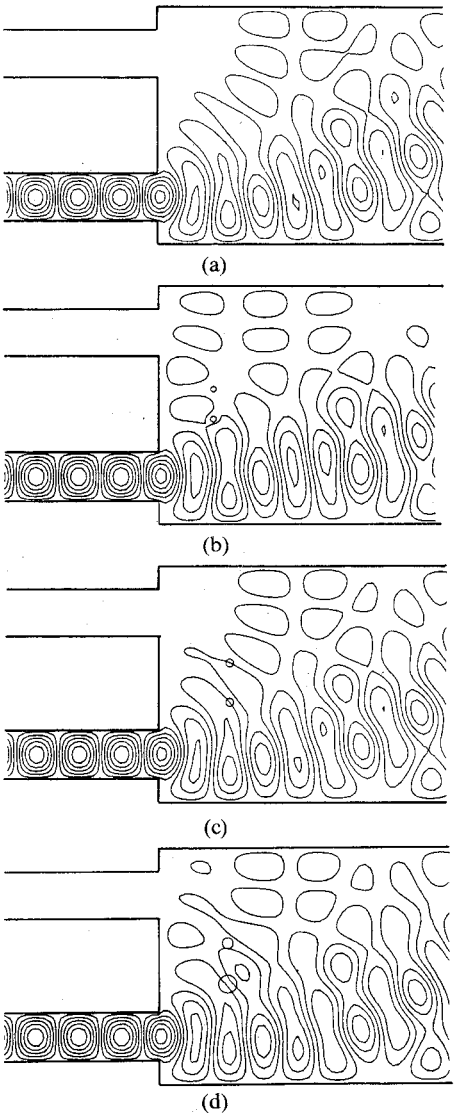

Fig. 8. Magnetic field in the symmetric rectangular waveguide branching from Fig. 3(b) and Fig. 7 at $f = 9.84$ GHz. (a) Without posts: $|S_{11}| = -24$ dB, $|S_{21}| = -38$ dB. (b) With two metallic posts: $|S_{11}| = -34$ dB, $|S_{21}| = -34$ dB. (c) With two Teflon posts: $|S_{11}| = -26$ dB, $|S_{21}| = -75$ dB. (d) With two asymmetric Teflon posts: $|S_{11}| = -35$ dB, $|S_{21}| = -35$ dB.

wave. Dielectric obstacles show a better detachment of fields at the discontinuity. So the Teflon posts yield better optimization results than the metallic posts.

V. Conclusions

As available computing power increases, the combination of the mode matching method and mathematical programming leads to an effective method for optimization of microwave devices. The method is demonstrated by applying nonlinear unconstrained minimization techniques to a rectangular step discontinuity with cylindrical obstacles and by using objective weighting to transform the vector optimization problem appearing in the case of the rectangular waveguide branching.

Acknowledgment

The authors thankfully acknowledge the support given by Prof. Dr.-Ing. G. Piefke.

References

[1] H. Schmiedel, *Berechnug und Messung von Diskontinuitäten im Rechteckhohlleiter unter besonderer Berücksichtigung der Analyse und Synthese von Modenkopplern*, Fortschrittberichte der VDI Zeitschriften, Düsseldorf, 1983.
[2] H. Schmiedel, "Feldtheoretisch Analyse und Synthese von Modenkopplern," *Frequenz*, vol. 37, pp. 207–214, 1983.
[3] K.-H. Waegel, "Die Rechteckhohlleitergabel als Vieltypwellenleiter," *NTZ Archiv*, vol. 5, pp. 53–56, 1983.
[4] G. Piefke, *Feldtheorie III*. Mannheim: Bibl. Inst., 1977.
[5] K. Pfeiffer, *Untersuchung einer Hohlleiterverzweigung*, Diplomarbeit am Fachgebiet Theoretische Elektrotechnik der Technischen Hochschule Darmstadt, Darmstadt, 1983.
[6] R. Gesche, *Kreiszylindrische Streukörper im Rechteckhohlleiter*, Darmstädter Dissertation D17, Darmstadt, 1986.
[7] R. Gesche and N. Löchel, "Scattering by a lossy dielectric cylinder in a rectangular waveguide," *IEEE Trans. Microwave Theory Tech.*, vol. 36, pp. 137–144, 1988.
[8] R. Gesche and N. Löchel, "Two cylindrical obstacles in a rectangular waveguide—Resonances and filter applications," *IEEE Trans. Microwave Theory Tech.*, vol. 37, pp. 962–968, June 1989.
[9] S. Russenschuck, *Berechnung und Optimierung des Reflexions- und Übersprechverhaltens einer Hohlleiterverzweigung mit kreiszylindrischen Streukörpern*, Diplomarbeit am Fachgebeiet Theoretische Elektrotechnik der Technischen Hochschule Darmstadt, Darmstadt, 1986.
[10] D. M. Himmelblau, *Applied Nonlinear Programming*. New York: McGraw-Hill, 1972.
[11] H. G. Jacob, *Rechnergestützte Optimierung statischer und dynamischer Systeme*. Berlin, Heidelberg, New York: Springer, 1982.
[12] J. L. Kuester and J. H. Mize, *Optimization Techniques with Fortran*. New York: McGraw-Hill, 1973.
[13] W. Stadler, "Preference Optimality and Application of Pareto-Optimality," in *Multicriterion Decision Making*, A. Marzollo and G. Leitman, Eds. (CISM Courses and Lectures. Berlin, Heidelberg, New York: Springer, 1975.

Roland Gesche (M'88) was born in Berlin, Germany, on June 18, 1957. He received the Diplom-Ingenieur and the Doktor-Ingenieur degrees from the Technical University of Darmstadt, Germany, in 1982 and 1986, respectively.

From 1982 to 1987 he was employed as a research assistant at the Technical University of Darmstadt, where he was engaged in the theoretical investigation of microwave structures. Since 1987, he has been engaged in the development of high-frequency and microwave equipment for physical vapor deposition and plasma etching processes at Leybold AG, Alzenau, West Germany.

Stephan Russenschuck (M'87) was born in Rüsselsheim, West Germany, on April 27, 1961. He studied theoretical electrical engineering at the Technical University of Darmstadt, Germany, and received the Dipl.-Ing. degree in 1986.

Since 1986 he has been employed as a research assistant at the Technical University of Darmstadt, where he is engaged in the application of mathematical optimization in numerical field calculations.